

Radiative B decays to the axial K mesons at next-to-leading order

Jong-Phil Lee*

Department of Physics and IPAP, Yonsei University, Seoul, 120-749, Korea

Abstract

We calculate the branching ratios of $B \rightarrow K_1\gamma$ at next-to-leading order (NLO) of α_s where K_1 is the orbitally excited axial vector meson. The NLO decay amplitude is divided into the vertex correction and the hard spectator interaction part. The one is proportional to the weak form factor of $B \rightarrow K_1$ transition while the other is a convolution between light-cone distribution amplitudes and hard scattering kernel. Using the light-cone sum rule results for the form factor, we have $\mathcal{B}(B^0 \rightarrow K_1^0(1270)\gamma) = (0.828 \pm 0.335) \times 10^{-5}$ and $\mathcal{B}(B^0 \rightarrow K_1^0(1400)\gamma) = (0.393 \pm 0.151) \times 10^{-5}$.

Typeset using REVTEX

*e-mail: jplee@phya.yonsei.ac.kr

I. INTRODUCTION

Radiative B decays into Kaons provide abundant issues for both theorists and experimentalists. After the first measurement at CLEO, $B \rightarrow K^* \gamma$ is now also measured in Belle and BaBar:

$$\mathcal{B}(B^0 \rightarrow K^{*0} \gamma) = \begin{cases} (4.09 \pm 0.21 \pm 0.19) \times 10^{-5} & \text{Belle [1]} \\ (4.23 \pm 0.40 \pm 0.22) \times 10^{-5} & \text{BaBar [2]} \\ (4.55 \pm 0.70 \pm 0.34) \times 10^{-5} & \text{CLEO [3]} \end{cases}, \quad (1)$$

$$\mathcal{B}(B^+ \rightarrow K^{*+} \gamma) = \begin{cases} (4.40 \pm 0.33 \pm 0.24) \times 10^{-5} & \text{Belle [1]} \\ (3.83 \pm 0.62 \pm 0.22) \times 10^{-5} & \text{BaBar [2]} \\ (3.76 \pm 0.86 \pm 0.28) \times 10^{-5} & \text{CLEO [3]} \end{cases}. \quad (2)$$

Theoretical advances in $B \rightarrow K^* \gamma$ have been noticeable for a decade. QCD corrections at next-to-leading order (NLO) of $\mathcal{O}(\alpha_s)$ was already considered in [4–6]. Furthermore, relevant Wilson coefficients have been improved [7,8] up to three-loop calculations. Recent developments of the QCD factorization [9] helped one calculate the hard spectator contributions systematically in a factorized form through the convolution at the heavy quark limit [10–12]. $B \rightarrow K^* \gamma$ is also analyzed in the effective theories at NLO, such as large energy effective theory [13] and the soft-collinear effective theory (SCET) [14].

In addition to K^* , higher resonances of Kaon also deserve much attention. Especially, it was suggested that $B \rightarrow K_{\text{res}} (\rightarrow K \pi \pi) \gamma$ can provide a direct measurement of the photon polarization [15]. In particular, it was shown that $B \rightarrow K_1(1400) \gamma$ can produce large polarization asymmetry of $\approx 33\%$ in the standard model. In the presence of anomalous right-handed couplings, the polarization can be severely reduced in the parameter space allowed by current experimental bounds of $B \rightarrow X_s \gamma$ [16]. It was also argued that the B factories can now make a lot of $B \bar{B}$ pairs enough to check the anomalous couplings through the measurement of the photon polarization.

As for the axial K_1 , unfortunately, current measurements give only upper bounds for $B \rightarrow K_1 \gamma$. For the decays of $B \rightarrow K_2(1430) \gamma$, CLEO and the B factories have reported the branching ratios

$$\mathcal{B}(B \rightarrow K_2^* \gamma) = (1.66^{+0.59}_{-0.53} \pm 0.13) \times 10^{-5} \text{ CLEO [3]}, \quad (3)$$

$$\mathcal{B}(B^0 \rightarrow K_2^{*0} \gamma) = \begin{cases} (1.3 \pm 0.5 \pm 0.1) \times 10^{-5} & \text{Belle [17]} \\ (1.22 \pm 0.25 \pm 0.11) \times 10^{-5} & \text{BaBar [18]} \end{cases}, \quad (4)$$

$$\mathcal{B}(B^+ \rightarrow K_2^{*+} \gamma) = (1.44 \pm 0.40 \pm 0.13) \times 10^{-5} \text{ BaBar [18]}. \quad (5)$$

Since the higher resonant Kaons are rather heavy $\gtrsim 1$ GeV, it is quite natural and attractive to consider them as heavy mesons. The advent of heavy quark effective theory (HQET) provoked many studies. Although the HQET simplifies the analysis by reducing number of the independent form factors involved, other non-perturbative methods are needed to complete the phenomenological explanation. These HQET-based analyses include HQET-ISGW (Isgur-Scora-Grinstein-Wise) [19] and HQET-NRQM (Non-Relativistic Quark Model) [20]. Other model calculations have been done in [21–24].

In this paper, the branching ratios of $B \rightarrow K_1 \gamma$ at NLO of α_s are calculated. We adopt the QCD factorization framework where the hard spectator interactions are described by

the convolution between the hard-scattering kernel and the light-cone distribution amplitudes (DA) at the heavy quark limit. All the non-perturbative nature are encapsulated in the DA while the hard kernel is perturbatively calculable. Basically, $B \rightarrow K_1\gamma$ shares many things with $B \rightarrow K^*\gamma$. Only the difference is the DA for the daughter mesons. Vector and axial vector mesons are distinguished by the γ_5 in the gamma structure of DA and some non-perturbative parameters. But the presence of γ_5 does not alter the calculation, giving the same result for the perturbative part. As for the non-perturbative parameters, the decay constant is most important. If higher twist terms are included, the Gegenbauer moments in the Gegenbauer expansion are also process dependent. We will not consider higher twists for simplicity.

Another NLO contributions are the vertex corrections to the relevant operators. They are all proportional to the leading operator O_7 . The matrix elements of O_7 are parameterized by several form factors. For the radiative decays where the emitted photons are real, only one form factor enters the decay amplitude. However, other non-perturbative calculation is needed for the value of the form factor. We use the light-cone sum rule (LCSR) results for it [25].

Thus at NLO, $B \rightarrow K^*\gamma$ and $B \rightarrow K_1\gamma$ are characterized by the weak form factor $F_+^{V(A)}$ and decay constant, plugged by the common perturbative and kinematical factors. With $\mathcal{B}(B \rightarrow K^*\gamma)$ at hand, near future measurements of $B \rightarrow K_1\gamma$ will check this structure.

The paper is organized as follows. General setup and leading contribution to $B \rightarrow K_1\gamma$ are given in the next Section. Section III is devoted to the NLO corrections. The resulting branching ratios and related discussions appear in Sec. IV. We conclude in Sec. V.

II. LEADING ORDER CONTRIBUTION

Let us start with the effective Hamiltonian for $b \rightarrow s\gamma$,

$$\mathcal{H}_{\text{eff}}(b \rightarrow s\gamma) = -\frac{G_F}{\sqrt{2}} V_{tb} V_{ts}^* \sum_{i=1}^8 C_i(\mu) O_i(\mu) , \quad (6)$$

where

$$\begin{aligned} O_1 &= (\bar{s}_i c_j)_{V-A} (\bar{c}_j b_i)_{V-A} , \\ O_2 &= (\bar{s}_i c_i)_{V-A} (\bar{c}_j b_j)_{V-A} , \\ O_3 &= (\bar{s}_i b_i)_{V-A} \sum_q (\bar{q}_j q_j)_{V-A} , \\ O_4 &= (\bar{s}_i b_j)_{V-A} \sum_q (\bar{q}_j q_i)_{V-A} , \\ O_5 &= (\bar{s}_i b_i)_{V-A} \sum_q (\bar{q}_j q_j)_{V+A} , \\ O_6 &= (\bar{s}_i b_j)_{V-A} \sum_q (\bar{q}_j q_i)_{V+A} , \\ O_7 &= \frac{em_b}{8\pi^2} \bar{s}_i \sigma^{\mu\nu} (1 + \gamma_5) b_i F_{\mu\nu} , \end{aligned}$$

$$O_8 = \frac{g_s m_b}{8\pi^2} \bar{s}_i \sigma^{\mu\nu} (1 + \gamma_5) T_{ij}^a b_j G_{\mu\nu}^a . \quad (7)$$

Here i, j are color indices, and we neglect the CKM element $V_{ub}V_{us}^*$ as well as the s -quark mass. The leading contribution to $B \rightarrow K_1\gamma$ comes from the electromagnetic operator O_7 as shown in Fig. 1. The matrix element of O_7 is described by the transition form factors $F_{\pm,0}^A$ which are defined by

$$\begin{aligned} & \langle K_1(p', \epsilon) | \bar{s}i\sigma_{\mu\nu}q^\nu b | B(p) \rangle \\ &= F_+^A(q^2) \left[(\epsilon^* \cdot q)(p + p')_\mu - \epsilon_\mu^*(p^2 - p'^2) \right] + F_-^A(q^2) \left[(\epsilon^* \cdot q)q_\mu - \epsilon_\mu^* q^2 \right] \\ &+ \frac{F_0^A(q^2)\epsilon^* \cdot q}{m_B m} \left[(p^2 - p'^2)q_\mu - (p + p')_\mu q^2 \right], \end{aligned} \quad (8a)$$

$$\langle K_1(p', \epsilon) | \bar{s}i\sigma_{\mu\nu}\gamma_5 q^\nu b | B(p) \rangle = iF_+^A(q^2)\epsilon_{\mu\nu\alpha\beta}\epsilon^{*\nu}q^\alpha(p + p')^\beta, \quad (8b)$$

where m and ϵ^μ are the mass and polarization vector of K_1 , respectively, and $q = p - p'$ is the photon momentum. In case of real photon emission ($q^2 = 0$), only F_+^A is involved as

$$\begin{aligned} \langle O_7 \rangle_A &\equiv \langle K_1(p', \epsilon) \gamma(q, e) | O_7 | B(p) \rangle \\ &= \frac{em_b}{4\pi^2} F_+^A(0) \left[\epsilon^* \cdot q(p + p') \cdot e^* - \epsilon^* \cdot e^*(p^2 - p'^2) + i\epsilon_{\mu\nu\alpha\beta}\epsilon^{*\mu}\epsilon^{*\nu}q^\alpha(p + p')^\beta \right], \end{aligned} \quad (9)$$

with e^μ being the photon polarization vector. The decay rate is straightforwardly obtained to be

$$\Gamma(B \rightarrow K_1\gamma) = \frac{G_F^2 \alpha m_b^2 m_B^3}{32\pi^4} |V_{tb}V_{ts}^*|^2 \left(1 - \frac{m^2}{m_B^2} \right)^3 |F_+^A|^2 |C_7^{\text{eff}(0)}|^2, \quad (10)$$

where α is the fine-structure constant and $C_7^{\text{eff}(0)}$ is the effective Wilson coefficient at leading order.

III. MATRIX ELEMENTS AT NEXT-TO-LEADING ORDER OF $\mathcal{O}(\alpha_S)$

At next-to-leading order of α_s , there are other contributions from the operators O_2 and O_8 . We simply neglect the annihilation topologies. Explicitly, the decay amplitude \mathcal{A} is given by

$$\mathcal{A}(B \rightarrow K_1\gamma) = -\frac{G_F}{\sqrt{2}} V_{tb} V_{ts}^* (C_7^{\text{eff}} \langle O_7 \rangle + C_2 \langle O_2 \rangle + C_8^{\text{eff}} \langle O_8 \rangle), \quad (11)$$

where $\langle O_i \rangle \equiv \langle K_1\gamma | O_i | B \rangle$. Every $\langle O_i \rangle$ has its vertex correction $\langle O_i \rangle_{VC}$ and hard spectator interaction term $\langle O_i \rangle_{HS}$ as shown in Figs. 2 and 3;

$$\langle O_i \rangle = \langle O_i \rangle_{VC} + \langle O_i \rangle_{HS}. \quad (12)$$

As for $\langle O_7 \rangle$, all the subleading contributions shown in Fig. 2 are absorbed into the form factor F_+^A while the corresponding Wilson coefficient C_7^{eff} contains its NLO part,

$$C_7^{\text{eff}}(\mu) = C_7^{\text{eff}(0)}(\mu) + \frac{\alpha_s(\mu)}{4\pi} C_7^{\text{eff}(1)}(\mu) . \quad (13)$$

On the other hand, the leading order $C_2^{(0)}$ and $C_8^{(0)}$ are sufficient for C_2 and C_8 since O_2 and O_8 contributions begin at NLO.

The vertex corrections are directly proportional to the form factor F_+^A . They are given by (Fig. 3) [6,8]

$$\langle O_2 \rangle_{VC} = \frac{\alpha_s}{4\pi} \langle O_7 \rangle \left(\frac{416}{81} \ln \frac{m_b}{\mu} + r_2 \right) , \quad (14)$$

$$\langle O_8 \rangle_{VC} = \frac{\alpha_s}{4\pi} \langle O_7 \rangle \left[-\frac{32}{9} \ln \frac{m_b}{\mu} + \frac{4}{27} (33 - 2\pi^2 + 6i\pi) \right] , \quad (15)$$

where

$$\begin{aligned} r_2 = & \frac{2}{243} \left\{ -833 + 144\pi^2 z^{3/2} \right. \\ & + \left[1728 - 180\pi^2 - 1296\zeta(3) + (1296 - 324\pi^2)L + 108L^2 + 36L^3 \right] z \\ & + \left[648 + 72\pi^2 + (432 - 216\pi^2)L + 36L^3 \right] z^2 + \left[-54 - 84\pi^2 + 1092L - 756L^2 \right] z^3 \left. \right\} \\ & + i \frac{16\pi}{81} \left\{ -5 + \left[45 - 3\pi^2 + 9L + 9L^2 \right] z + \left[-3\pi^2 + 9L^2 \right] z^2 + \left[28 - 12L \right] z^3 \right\} , \end{aligned} \quad (16)$$

with $z \equiv m_c^2/m_b^2$, $L \equiv \ln z$, and $\zeta(x)$ being the Liemann ζ -function.

Hard spectator corrections are well described by the convolution between the hard kernel $T_i(\xi, u)$ and the light-cone distribution amplitudes of the involved mesons, $\Phi_B(\xi)$ and $\Phi_A(u)$, in the heavy quark limit;

$$\langle O_i \rangle_{HS} = \int_0^1 d\xi du \Phi_B(\xi) T_i(\xi, u) \Phi_A(u) . \quad (17)$$

The light-cone distribution amplitudes are defined by

$$\langle 0 | b(0) \bar{q}'(z) | B(p) \rangle = \frac{if_B}{4} (\not{p} + m_B) \gamma_5 \int_0^1 d\xi e^{-i\xi p + z_-} \left[\Phi_{B1}(\xi) + \not{\xi} \Phi_{B2}(\xi) \right] , \quad (18a)$$

$$\langle A(p', \epsilon) | q(z) \bar{q}(0) | 0 \rangle = \frac{f_A^\perp}{4} \gamma_5 \sigma^{\mu\nu} \epsilon_\mu p'_\nu \int_0^1 du e^{i\bar{u} p' \cdot z} \Phi_A^\perp(u) , \quad (\bar{u} \equiv 1 - u) \quad (18b)$$

where $\bar{n}^\mu = (1, 0, 0, -1)$ is parallel to the outgoing meson. To calculate the hard spectator contributions, following kinematics for Fig. 2 is adopted:

$$\begin{aligned} p_b^\mu &= m_b v^\mu , \\ l^\mu &= \frac{l_+}{2} n^\mu + l_\perp^\mu + \frac{l_-}{2} \bar{n}^\mu , \\ q^\mu &= \omega n^\mu \quad (\omega \simeq m_B/2) , \\ k_1^\mu &\simeq u E \bar{n}^\mu + k_\perp^\mu + \mathcal{O}(k_\perp^2) , \\ k_2^\mu &\simeq \bar{u} E \bar{n}^\mu - k_\perp^\mu + \mathcal{O}(k_\perp^2) \quad (E \simeq m_B/2) , \end{aligned} \quad (19)$$

where $n^\mu = (1, 0, 0, 1)$ and u is the relative energy fraction.

Direct calculation of each diagram in Fig. 4 plugged with Eq. (18) yields

$$\langle O_2 \rangle_{HS} = \frac{\langle O_7 \rangle_A}{F_+^A(0)} \frac{4\pi\alpha_s C_F}{N_c} \frac{f_B f_A^\perp}{m_b m_B} \left[\frac{1}{12} \langle u^{-1} \Delta F_1(z_1^{(c)}) \rangle_\perp + \frac{3}{16} Q_{sp} \langle \bar{u}^{-1} \Delta F_1(z_0^{(c)}) \rangle_\perp - \frac{1}{12} \langle \xi^{-1} \rangle_1 \langle \bar{u}^{-1} \Delta i_5(z_0^{(c)}, z_1^{(c)}, 0) \rangle_\perp - \frac{1}{3} \langle \bar{u}^{-1} \Delta i_{25}(z_0^{(c)}, z_1^{(c)}, 0) \rangle_\perp \right], \quad (20)$$

$$\langle O_8 \rangle_{HS} = \frac{\langle O_7 \rangle_A}{F_+^A(0)} \frac{4\pi\alpha_s C_F}{N_c} \frac{f_B f_A^\perp}{m_B^2} \left[\frac{1}{12} \langle u^{-1} \rangle_\perp \langle \xi^{-1} \rangle_1 + \frac{Q_{sp}}{8} (\langle \bar{u}^{-1} \rangle_\perp + 2 \langle \bar{u}^{-2} \rangle_\perp) \right]. \quad (21)$$

Here N_c is the number of color with $C_F = \frac{N_c^2 - 1}{2N_c}$, and Q_{sp} is the electric charge of the spectator quark. The expectation values over the distribution amplitudes are defined by

$$\langle f(u) \rangle_\perp \equiv \int_0^1 du f(u) \Phi_A^\perp(u), \quad (22a)$$

$$\langle \xi^N \rangle_1 \equiv \int_0^1 d\xi \xi^N \Phi_{B1}(\xi). \quad (22b)$$

Relevant functions ΔF_1 , Δi_5 , and Δi_{25} as well as the arguments $z_{0,1}^{(f)}$ are given in [13,26].

IV. BRANCHING RATIOS FOR $B \rightarrow K_1\gamma$

The branching ratio of $B \rightarrow K_1\gamma$ is simply given by

$$\mathcal{B}(B \rightarrow K_1\gamma) = \tau_B \frac{G_F^2 \alpha m_b^2 m_B^3}{32\pi^4} \left(1 - \frac{m_A^2}{m_B^2}\right)^3 |F_+^A(0)|^2 |V_{tb} V_{ts}^*|^2 |C_7^{\text{eff}}(\mu_b) + A_{VC} + A_{HS}|^2. \quad (23)$$

At the heavy quark limit,

$$A_{VC} = \frac{\alpha_s(\mu_b)}{4\pi} \left\{ C_8^{\text{eff}}(\mu_b) \left[-\frac{32}{9} \ln \frac{m_b}{\mu_b} + \frac{4}{27} (33 - 2\pi^2 + 6i\pi) \right] + C_2(\mu_b) \left[\frac{416}{81} \ln \frac{m_b}{\mu_b} + r_2 \right] \right\},$$

$$A_{HS} = \frac{4\pi\alpha_s(\mu_H) C_F}{N_c} \frac{\lambda_B f_B f_A^\perp}{m_B F_+^A(0)} \left\{ C_8^{\text{eff}}(\mu_H) \frac{1}{12} \langle u^{-1} \rangle_\perp - C_2(\mu_H) \frac{1}{12} \left\langle \frac{\Delta i_5(z_0^{(c)}, 0, 0)}{\bar{u}} \right\rangle_\perp \right\}, \quad (24)$$

where the negative moment of Φ_{B1} is parameterized by $\lambda_B \sim \mathcal{O}(\Lambda_{\text{QCD}})$ as

$$\int_0^1 d\xi \frac{\Phi_{B1}(\xi)}{\xi} \equiv \frac{m_B}{\lambda_B}. \quad (25)$$

The renormalization scale is fixed at $\mu = \mu_b = \mathcal{O}(m_b)$ for the vertex corrections while for the hard spectator interactions, $\mu = \mu_H \sim \sqrt{\Lambda_{\text{QCD}} m_b}$. In the following analysis, we set $\mu_b = m_b$ and $\mu_H = \sqrt{\Lambda_H m_b}$ where $\Lambda_H = 0.5$ GeV.

The scale dependence of $\langle O_7 \rangle$ is absorbed into the product of b -quark mass and the form factor; [12]

$$(m_b \cdot F_+^A)[\mu] = (m_b \cdot F_+^A)[m_b] \left(1 + \frac{\alpha_s(\mu)}{4\pi} \frac{32}{3} \ln \frac{m_b}{\mu} \right). \quad (26)$$

Other input values are summarized in Table I. Contrary to the $B \rightarrow K^* \gamma$, there are few reliable values for $F_+^A(0)$ and f_A^\perp both in theory and experiment in the literature. We adopt the results from the light-cone sum rules by Safir, whose values are listed in Table II. In Table III, each contributions to the decay amplitudes is listed from the central values of Tables I and II. Note that the NLO corrections contribute positively, except $C_7^{\text{eff}(1)}$. Reference scale for the present analysis is

$$(\mu_b, \mu_H) = (m_b(m_b), \sqrt{\Lambda_H m_b(m_b)}) = (4.2 \text{ GeV}, 1.45 \text{ GeV}). \quad (27)$$

As a comparison, results for another scale $(\mu_b, \mu_H) = (m_{b,PS}, (m_b(m_b)))$ are also given in Table III, where $m_{b,PS} = 4.6$ GeV is the so-called potential-subtracted mass [27]. It should be emphasized that in Table III, C_7^{eff} and A_{VC} are process independent, and encodes QCD effects only. On the other hand, A_{HS} contains the key information of the outgoing meson. Although $F_+^A(0)$ in A_{HS} is canceled, non-perturbative properties of daughter meson still remain in f_A^\perp and $\langle \cdots \rangle_\perp$. When averaging over $\Phi_A^\perp(u)$, process dependence is encapsulated in the coefficients of the Gegenbauer expansion, which vanish at $\mu \rightarrow \infty$. We simply neglect the expansion here, retaining Φ_A^\perp as its asymptotic form

$$\Phi_A^\perp(u) \approx \Phi_A^{\perp(as)}(u) = 6u\bar{u}. \quad (28)$$

Keeping the hadronic parameters specifically, we have

$$\mathcal{B}(B^0 \rightarrow K_1^0 \gamma) = 0.003 \times \left(1 - \frac{m^2}{m_B^2} \right)^3 \times |F_+^A(0)(-0.385 - i0.014) + f_A^\perp(-0.024 - i0.022)|^2. \quad (29)$$

Final results for the decay amplitudes and the branching ratios are listed in Table IV. Uncertainties in the branching ratios are from those in the form factor. For the charged modes, one has only to multiply the life-time ratio τ_{B^\pm}/τ_{B^0} to the above equation.

In Eq. (29), the coefficient of $F_+^A(0)$ is $C_7^{\text{eff}}(\mu_b) + A_{VC}(\mu_b)$, while that of f_A^\perp is $A_{HS}(\mu_H) \times F_+^A(0)/f_A^\perp$. Since the presence of γ_5 in Eq. (18b) does not change the trace calculation for getting Eq. (20) and the form of $\Phi_A^{\perp(as)}$ is universal, the numerics in Eq. (29) are common to both $B \rightarrow K_V \gamma$ and $B \rightarrow K_A \gamma$, irrespective of the species of K_V or K_A . This is quite an interesting point considering the fact that the measurements for $B \rightarrow K_A \gamma$ are near at hand. Most of all, the mass hierarchy of $m_{K^*} < 1 \text{ GeV} < m_{K_1}$ might impose some doubts about the common framework for both K^* and K_1 . Actually, the scale 1 GeV is very delicate because the chiral symmetry is broken around it. Recall that in calculating the hard spectator interactions it is assumed that the axial Kaon is nearly massless. Although the assumption is acceptable for $m_{K_1} \ll m_B$, it is also possible that nonzero mass effects are sizable. So far, there is no systematics to deal with it. The compatibility of Eq. (29) with experimental observations for both $B \rightarrow K^* \gamma$ and $B \rightarrow K_1 \gamma$ will cast some clues to this issue. In the kinematically opposite limit where K_1 is very heavy, Ref. [19,20] predicted branching ratios of higher Kaon resonances. Their results as well as those from other methods are

listed in Table V for a comparison. In the heavy quark scheme, hard spectator interaction is inconceivable since almost all the momentum of initial heavy meson is transferred to the final one. Typical scale of interaction with the spectator is $\sim \Lambda_{\text{QCD}}$ where the perturbative approach breaks down. Thus checking the validity of hard spectator contribution plays an important role in determining which approach is more reliable.

The biggest uncertainty in theoretical prediction lies in calculation of the form factor F_+^A . QCD sum rule is among the most reliable. But recent analysis on $B \rightarrow K^* \gamma$ reveals that LCSR results for the relevant form factor lead to a very large branching ratio compared to the measured one [13]. Unfortunately, there is no way to explain the discrepancy up to now. The will-be-extracted values of F_+^A from the experiments, therefore, provide much interest to see whether the LCSR predicts larger form factors again.

Another issue of $B \rightarrow K_1 \gamma$ is mixing. If experiments measure very different values of $\mathcal{B}(B \rightarrow K_1(1270)\gamma)$ and $\mathcal{B}(B \rightarrow K_1(1400)\gamma)$, then the maximal mixing of K_{1A} and K_{1B} , which correspond to 3P_1 and 1P_1 quark model states respectively, is more favored [24]. One can be about 40 times larger than the other.

Present analysis is done at the heavy quark limit, at NLO of α_s , and at the leading twist of the distribution amplitudes for the involved mesons. At the heavy quark limit, only the terms proportional to $\langle \xi^{-1} \rangle_1 \sim \mathcal{O}(1/\Lambda_{\text{QCD}})$ survive. And the NLO α_s effects are,

$$\frac{|C_7^{\text{eff}(0)}|^2}{|C_7^{\text{eff}} + A_{VC} + A_{HS}|^2} \approx 62\% , \quad (30)$$

for both $K_1(1270)$ and $K_1(1400)$ at $(\mu_b, \mu_H) = (4.2 \text{ GeV}, 1.45 \text{ GeV})$. Higher twist effects are nontrivial and process dependent in general. For $B \rightarrow K^* \gamma$, the non-asymptotic correction of K^* at higher twist through the Gegenbauer moments to the operator O_8 amounts to $\sim -20\%$ [13]. Similar effects are expected in K_1 .

V. CONCLUSIONS

Radiative B decays to the Kaon resonances provide a rich laboratory to test the standard model and probe new physics. $B \rightarrow K^* \gamma$ is a well established process, and Belle and BaBar are now measuring the decay modes of higher resonances for the first time. In a theoretical side, deeper understandings have been accomplished for a decade. For example, relevant Wilson coefficients are known up to the three-loop level. The idea of the QCD factorization reduces model or process dependences. And various versions of effective theories of QCD such as HQET or SCET have simplified the analysis dramatically.

In this paper, radiative B decays to the axial Kaons are examined at NLO of $\mathcal{O}(\alpha_s)$. This was already done for K^* a few years ago, and many aspects are common. Especially, they share the same perturbative QCD part and only the weak form factor as well as some static properties of the final K_{res} discern the specific process, at the leading twist and heavy quark limit.

On the other hand, the largest uncertainty of theory is the form factor for which we used the LCSR calculations. Since the results of LCSR for $B \rightarrow K^*$ form factor turn out to be quite large compared to the experiments, the reliability is rather low. A clear explanation of the discrepancy will remain a good challenge. In this respect, near future measurements for

$B \rightarrow K_1\gamma$ and extraction of the form factor are quite exciting. They also check the possible mixing between 3P_1 and 1P_1 states to form physical $K_1(1270)$ and $K_1(1400)$.

Acknowledgements

This work was supported by the BK21 Program of the Korean Ministry of Education.

REFERENCES

- [1] Belle Collaboration, K. Abe *et al.*, BELLE-CONF-0319 (2003).
- [2] BaBar Collaboration, B. Aubert *et al.*, Phys. Rev. Lett. **88**, 101805 (2002).
- [3] CLEO Collaboration, T.E. Coan *et al.*, Phys. Rev. Lett. **84**, 5283 (2000).
- [4] J.M. Soares, Nucl. Phys. **B367**, 575 (1991); Phys. Rev. D **49**, 283 (1994).
- [5] C. Greub, H. Simma, and D. Wyler, Nucl. Phys. **B434**, 39 (1995); Erratum *ibid.* **444**, 447 (1995).
- [6] C. Greub, T. Hurth, and D. Wyler, Phys. Rev. D **54**, 3350 (1996).
- [7] K. Adel and Y. Yao, Phys. Rev. D **49**, 4945 (1994).
- [8] K. Chetyrkin, M. Misiak, and M. Münz, Phys. Lett. B **400**, 206 (1997).
- [9] M. Beneke, G. Buchalla, M. Neubert, and C.T. Sachrajda, Nucl. Phys. **B591**, 313 (2000).
- [10] M. Beneke and T. Feldmann, Nucl. Phys. **B592**, 3 (2001).
- [11] M. Beneke, T. Feldmann, and D. Siedel, Nucl. Phys. **B612**, 25 (2001).
- [12] S.W. Bosch and G. Buchalla, Nucl. Phys. **B621**, 459 (2002).
- [13] A. Ali and A.Ya. Parkhomenko, Eur. Phys. J. C **23**, 89 (2002).
- [14] J. Chay and C. Kim, Phys. Rev. D **68**, 034013 (2003).
- [15] M. Gronau, Y. Grossman, D. Pirjol, and A. Ryd, Phys. Rev. Lett. **88**, 051802 (2002); M. Gronau and D. Pirjol, Phys. Rev. D **66**, 054008 (2002).
- [16] J.-P. Lee, Phys. Rev. D **69**, 014017 (2004); *Proceeding of the 2nd ICFP 03, Seoul, Korea* [hep-ph/0312010].
- [17] Belle Collaboration, S. Nishida *et al.*, Phys. Rev. Lett. **89**, 231801 (2002).
- [18] BaBar Collaboration, A. Aubert *et al.*, [hep-ex/0308021].
- [19] A. Ali, T. Ohl, and T. Mannel, Phys. Lett. B **298**, 195 (1993).
- [20] S. Veseli and M.G. Olsson, Phys. Lett. B **367**, 309 (1996).
- [21] T. Altomari, Phys. Rev. D **37**, 677 (1998).
- [22] D. Atwood and A. Soni, Z. Phys. **64**, 241 (1994).
- [23] D. Ebert, R.N. Faustov, V.O. Galkin, and H. Toki, Phys. Rev. D **64**, 054001 (2001).
- [24] H.-Y. Cheng and C.-K. Chua, [hep-ph/0401141].
- [25] A.S. Safir, Eur. Phys. J. direct C **3**, 15 (2001).
- [26] H. Simma and D. Wyler, Nucl. Phys. **B344**, 283 (1990).
- [27] M. Beneke, Phys. Lett. B **434**, 115 (1998); M. Beneke, A. Signer, Phys. Lett. B **471**, 233 (1999).

FIGURE CAPTIONS

Fig. 1

Leading order contribution by operator O_7 .

Fig. 2

NLO corrections to O_7 . These diagrams are absorbed into the weak form factor F_+^A .

Fig. 3

Vertex corrections to the operators (a) O_2 and (b) O_8 . Crosses denote the possible attachment of the emitted photon.

Fig. 4

Hard spectator interactions to (a) O_2 and (b) O_8 . First diagrams are leading contributions at the heavy quark limit.

FIGURES

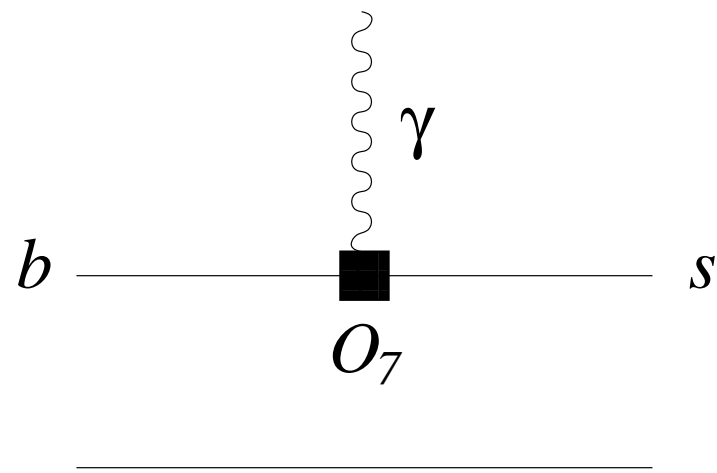


FIG. 1.

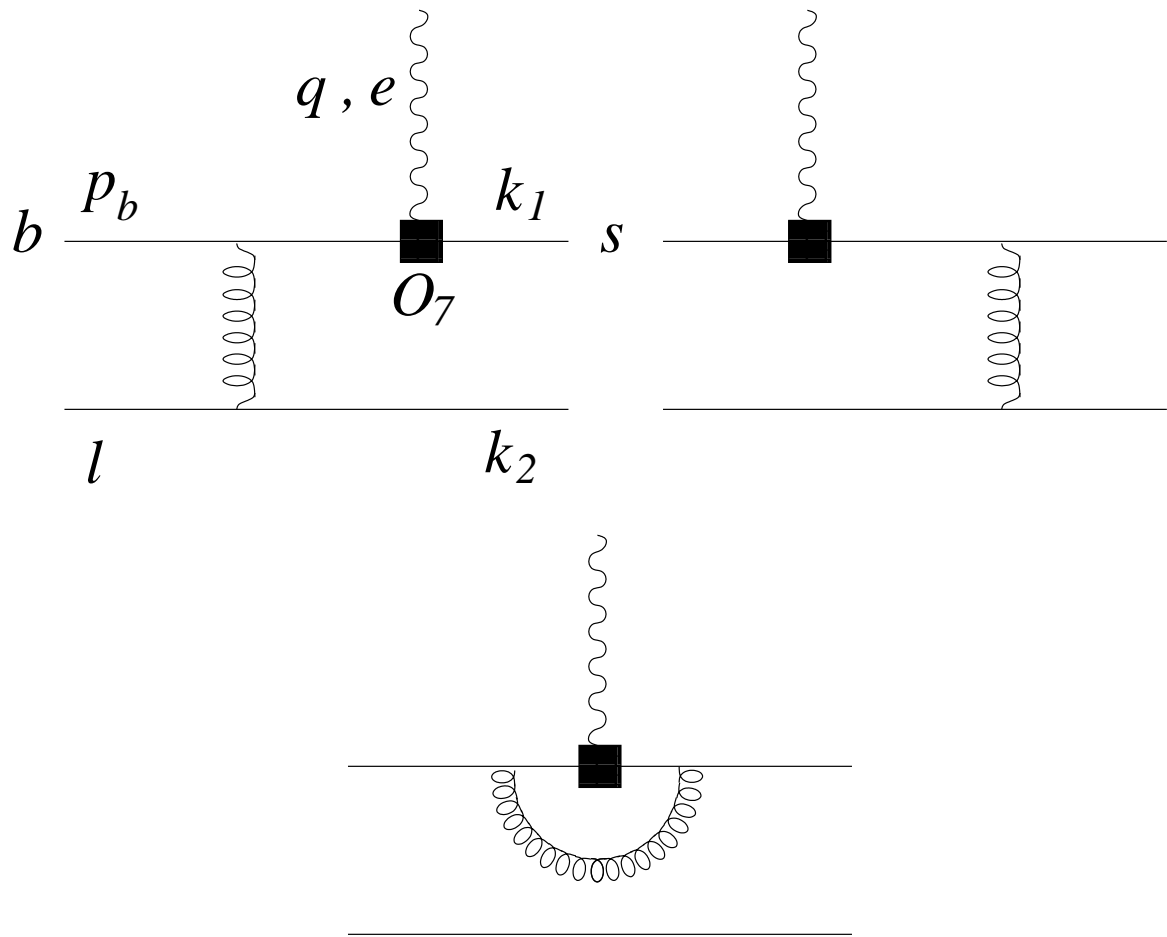
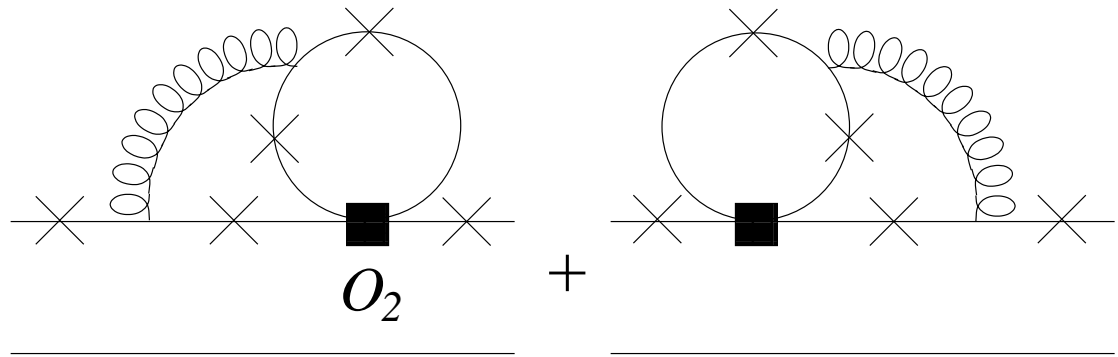
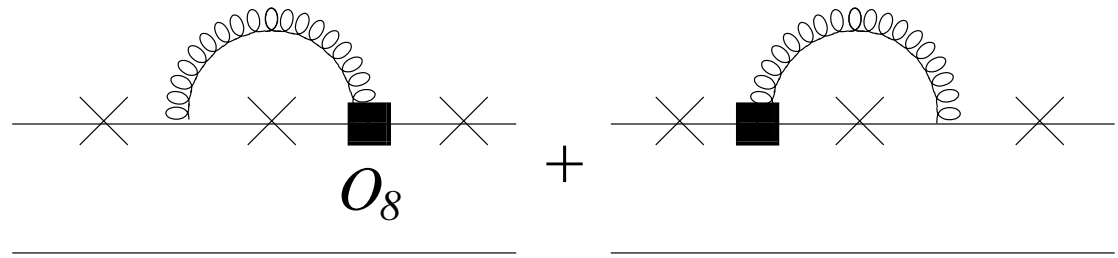


FIG. 2.



+

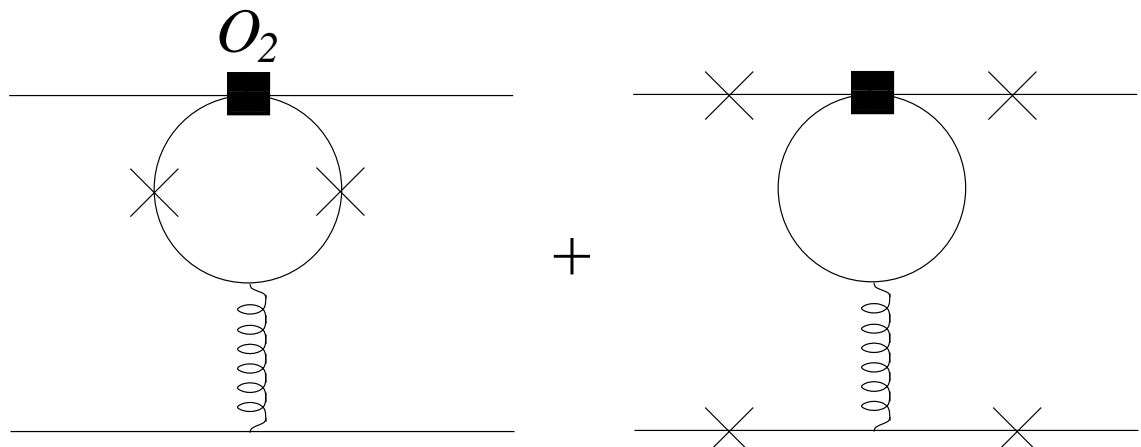
(a)



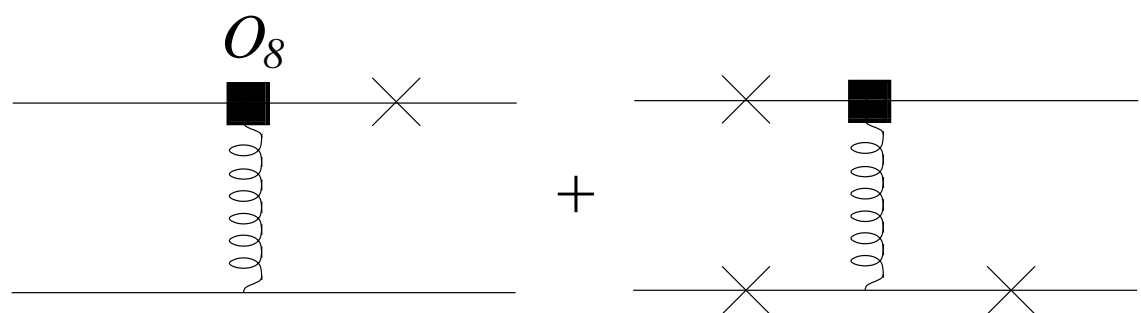
+

(b)

FIG. 3.



(a)



(b)

FIG. 4.

TABLES

TABLE I. Summary of input values

$ V_{tb}V_{ts}^* $	0.0396 ± 0.0020 [13]
τ_{B^+}	(1.674 ± 0.018) ps
τ_{B^0}	(1.542 ± 0.016) ps
m_B	5.28 GeV
f_B	0.18 GeV
λ_B	(0.35 ± 0.15) GeV
$m_b(m_b)$	4.2 GeV
$m_c(m_b)$	(1.3 ± 0.2) GeV

TABLE II. $F_+^A(0)$ and f_A from light-cone sum rules

Axial K_1	$K_1(1270)$	$K_1(1400)$
m_A	1.273 GeV	1.402 GeV
f_A	0.122 GeV	0.091 GeV
$F_+^A(0)$	0.14 ± 0.03	0.098 ± 0.02

TABLE III. Componential contributions to the decay amplitude

μ_b	$m_b(m_b) = 4.2$ GeV	$m_{b,PS} = 4.6$ GeV
$C_7^{\text{eff}(0)}(\mu_b)$	-0.321	-0.316
$C_7^{\text{eff}(1)}(\mu_b)$	0.602	0.522
$C_7^{\text{eff}}(\mu_b)$	-0.310	-0.307
$A_{VC}(\mu_b)$	$-0.075 - i0.014$	$-0.082 - i0.013$
μ_H	$\sqrt{\Lambda_H m_b(m_b)} = 1.45$ GeV	$m_b(m_b) = 4.2$ GeV
$A_{HS}^{K_1(1270)}(\mu_H)$	$-0.021 - i0.019$	$-0.013 - i0.013$
$A_{HS}^{K_1(1400)}(\mu_H)$	$-0.022 - i0.020$	$-0.014 - i0.013$

TABLE IV. Decay amplitudes and branching ratios for different scales

(μ_b, μ_H) (GeV)	(4.2, 1.45)	(4.2, 4.2)	(4.6, 1.45)	(4.6, 4.2)
$(C_7^{\text{eff}} + A_{VC} + A_{HS})_{K_1(1270)}$	$-0.406 - i0.033$	$-0.399 - i0.027$	$-0.410 - i0.033$	$-0.402 - i0.026$
$\mathcal{B}(B^0 \rightarrow K_1^0(1270)\gamma) \times 10^5$	0.828 ± 0.335	0.795 ± 0.329	0.814 ± 0.341	0.782 ± 0.335
$(C_7^{\text{eff}} + A_{VC} + A_{HS})_{K_1(1400)}$	$-0.408 - i0.034$	$-0.400 - i0.027$	$-0.412 - i0.034$	$-0.403 - i0.027$
$\mathcal{B}(B^0 \rightarrow K_1^0(1400)\gamma) \times 10^5$	0.393 ± 0.151	0.376 ± 0.148	0.386 ± 0.154	0.370 ± 0.150

TABLE V. Comparison with other results, in units of 10^{-5} .

Branching Ratio	$\mathcal{B}(B \rightarrow K_1(1270)\gamma)$	$\mathcal{B}(B \rightarrow K_1(1400)\gamma)$
JPL	0.828	0.393
Ref. [24]	$0.02 \sim 0.84$	$0.003 \sim 0.80$
Ref. [25]	0.493	0.241
Ref. [23]	0.45	0.78
Ref. [20]	1.20	0.58
Ref. [22]	$0.3 \sim 1.4$	$0.1 \sim 0.6$
Ref. [19]	$1.8 \sim 4.0$	$2.4 \sim 5.2$
Ref. [21]	1.1	0.7